

# Stabilized electron emission from silicon coated carbon nanotubes for a high-performance electron source

Je Hwang Ryu, Na Young Bae, and Hye Mi Oh

*Department of Information Display and Advanced Display Research Center, Kyung Hee University, Seoul 130-701, Korea*

Otto Zhou

*Department of Physics and Astronomy, University of North Carolina at Chapel Hill, North Carolina 27599-3255*

Jin Jang and Kyu Chang Park<sup>a)</sup>

*Department of Information Display and Advanced Display Research Center, Kyung Hee University, Seoul 130-701, Korea*

(Received 20 September 2010; accepted 18 February 2011; published 29 March 2011)

The authors show that carbon nanotubes (CNTs) coated with an amorphous silicon layer around their periphery show enhanced and stable electron emission. The CNT-field emitter array was grown on silicon substrate through a resist-assisted patterning process. The CNTs become coated with silicon from the substrate, which is etched and redeposited onto the CNTs. The authors obtained enhanced and stabilized electron emission from the silicon coated CNTs with a turn-on field of  $2 \text{ V}/\mu\text{m}$  at an emission current density of  $1 \mu\text{A}/\text{cm}^2$ . The structure and electron emission properties of the functionalized emitters are discussed. © 2011 American Vacuum Society. [DOI: 10.1116/1.3565428]

## I. INTRODUCTION

Carbon nanotubes (CNTs) exhibit remarkable properties that make them attractive for several nanoelectronic device applications including electron emitters. CNTs show characteristics, such as high aspect ratio, high thermal conductivity, and low chemical reactivity,<sup>1</sup> which make them suitable for the fabrication of x-ray tubes<sup>2,3</sup> and electron guns.<sup>4</sup> Stable field emission is the key requirement for CNTs in high-performance electron emission source applications.<sup>5</sup> Thus, there is a critical need for novel methods for growing CNTs. Electron sources for x-ray generation in tomosynthesis require an anode current that is greater than 100 mA.<sup>6</sup> Conventional CNT emitters do not meet this requirement because they rapidly degrade during high current operation. Stable and reliable electron emission is also necessary for extended operation.<sup>7</sup> For enhanced and stabilized electron emission, electron sources must strongly adhere to the substrate,<sup>8</sup> be robust under environmental stress, and possess sharp tips, which do not change and degrade during operation.

In this paper, we describe the growth of CNTs that become coated with amorphous silicon through reactions of the plasma species with the silicon substrate. The silicon coating can prevent chemical reactions of carbon with the gases in the environment and improve the stability of the CNTs. The structural and electron emission properties of the emitters and their stability are discussed.

## II. EXPERIMENT

The CNTs were grown using a resist-assisted patterning (RAP) process, which has been reported in detail

elsewhere.<sup>9,10</sup> For the RAP process, silicon substrates were used to grow the CNTs. The nickel catalyst layer was deposited on the silicon substrate using radio frequency magnetron sputtering.<sup>11</sup> The nickel catalyst layer was patterned using photoresist. The resist was patterned with  $3 \mu\text{m}$  sized islands with an island-to-island pitch of  $15 \mu\text{m}$ . The resist was not removed for seed formation and is required for CNT growth. The unwanted nickel catalyst was etched, and then the substrate was annealed in a high-temperature furnace. The annealing temperature and time in this study were  $600 \text{ }^\circ\text{C}$  and 30 min, respectively. After annealing, the nickel catalyst separated into small grains for the growth of the CNTs. CNTs can grow where there is carbon-network formation after the annealing process. Additional details about the RAP process can be found in a previously published report.<sup>9</sup>

The CNTs were grown in a triode direct current-plasma enhanced chemical vapor deposition (dc-PECVD) system with a mesh grid placed 10 mm above the substrate holder electrode. With this triode dc-PECVD system, the growth of CNTs is easily enhanced and inhibited by strong positive and negative bias voltages on the mesh electrode, respectively.<sup>12</sup> The CNT density and length can be changed easily by changing the mesh electrode bias and polarity. The mesh electrode bias voltage can alter the CNT growth mechanism by modifying the flux of the ions impinging on the substrate. A positive mesh bias increases the ion flux and electric field, resulting in increased CNT length and density (the higher the bias, the higher the length and density). However, a negative mesh bias, resulting in a reduced ion flux, reduces CNT density and growth rate probably because of catalyst particle poisoning by an amorphous carbon deposit that cannot be removed through sputtering.<sup>13</sup>

<sup>a)</sup>Author to whom correspondence should be addressed; electronic mail: kyupark@khu.ac.kr

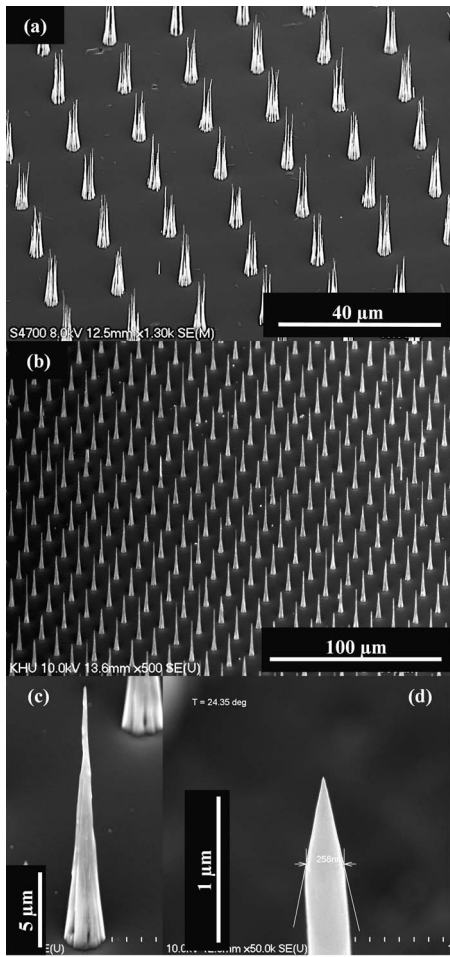


FIG. 1. SEM images of the CNT emitter array. (a) Vertically aligned CNT emitters. (b) Array of silicon coated CNT emitters with  $3 \mu\text{m}$  islands and  $15 \mu\text{m}$  pitch. (c) A magnified image of one silicon coated CNT emitter. (d) A magnified image of the tip apex of a silicon coated CNT emitter.

The structural properties of the silicon coated CNTs were characterized through field emission scanning electron microscopy (SEM) and transmission electron microscopy with energy dispersive x-ray spectroscopy (TEM-EDAX). The electron emission current was measured in dc mode with a diode structure under a pressure of  $1 \times 10^{-7}$  Torr.

### III. RESULTS AND DISCUSSION

In general, the initial CNTs aligned vertically and formed several multiwall CNTs on each nickel island. A SEM image of the vertically aligned CNTs is shown in Fig. 1(a). However, the structure changes with time, which results in the formation of silicon coated CNTs. SEM images of the silicon coated CNTs are shown in Figs. 1(b)–1(d). The structure of CNTs changes with growth time. As the growth time increases, the CNTs change in shape to become silicon coated. Figure 1(b) shows an entire array of CNT electron emitters that were grown for 120 min. The CNTs were  $3 \mu\text{m}$  in diameter and were pitched periodically every  $15 \mu\text{m}$ . The island size and pitch of the CNTs could be controlled through the catalyst fabrication process. The magnified image of a

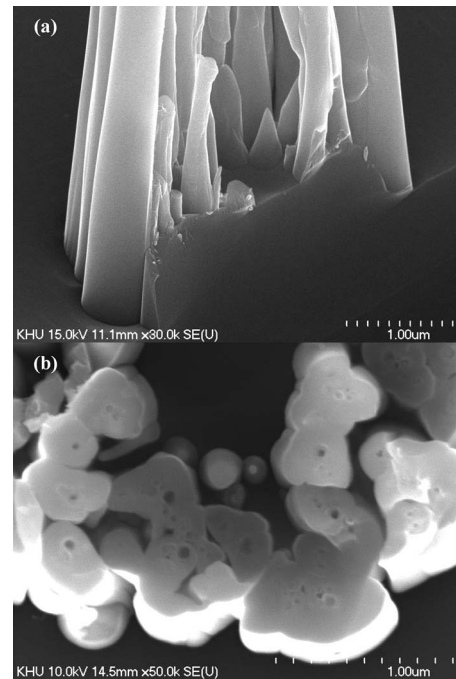


FIG. 2. SEM images of (a) cross-sectioned and (b) horizontally cross-sectioned silicon coated CNT emitter.

CNT is shown in Fig. 1(c). The figure clearly shows that the CNT had a sharp tip and a wide bottom; it was aligned vertically and well positioned in the predefined island area. The length of the CNT was approximately  $20 \mu\text{m}$ . As shown in Fig. 1(d), the diameter of the tip was in the nanometer range. The emitter tip was cone shaped with a sharp tip. The tip apex measured a few nanometers in diameter, and the diameter of the bottom region in contact with the substrate was equal to the prepatterned dot area of the  $3 \mu\text{m}$  island. The adhesion of conventional single CNTs onto the substrate is weak. However, the bottom contact area of the CNT emitters grown for 120 min exhibited multiple rods, as shown in Fig. 2(c). This is thought to increase the adhesion between the CNTs and the substrate.

The structure of the CNTs was unusual; there was one cone-shaped emitter with multiple rods in the bottom. To understand the structural properties, we obtained vertical and horizontal cross sections of the CNT for SEM measurements. Figure 2(a) shows a vertical cross-section image of the CNT emitter. The emitter shows strong and robust bonding with the silicon substrate. These CNT structures are robust in the sense that compared with conventional CNTs, they are more resistant to physical, electrical, and chemical stresses. Moreover, no CNTs were observed in the center of the  $3 \mu\text{m}$  dot. The reason of this was not clear. Figure 2(b) shows the cross-sectional SEM image of the CNT emitter. Several holes were observed in one rod. The diameter of the hole was several tens to hundreds of nanometers.

The structure of the emitters was studied further using TEM measurements. The TEM sample was prepared using a focused ion beam. The single emitter was horizontally cross sectioned with the ion beam and examined with TEM. The

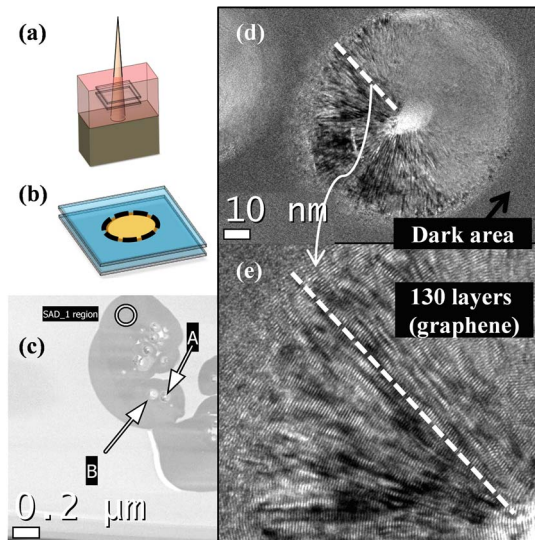


FIG. 3. (Color online) TEM images of silicon coated CNT emitters horizontally cross sectioned with a focused ion beam. (a) Sample preparation area. (b) Sample slice model image. (c) TEM image of the slice. (d) Magnified image of the bright area in (c). (e) Magnified image of (d).

sample preparation process is shown in Figs. 3(a) and 3(b). Figure 3(c) shows the TEM image of the single emitter after horizontal cross sectioning. Similar to the observation in Fig. 2(b), we observed a bright spot surrounded by a dark area. The bright spot in this TEM measurement represents a crystalline phase. The bright spot was magnified for structural analysis and is shown in Fig. 3(d). A crystalline structure with a 100 nm diameter was observed in the image. The diameter of the structure was similar to the CNTs grown through the conventional RAP process.<sup>4</sup> Furthermore, the TEM image also revealed a hole in the center of the spot, which indicated that the CNTs formed as tubular structures. As shown in Fig. 3(e), the CNT exhibits 130 layers. This measurement reveals that the various CNTs were surrounded by a thick amorphous layer (dark area). The amorphous layer grows continuously on the CNT surface with increasing growth time and surrounds each CNT after 120 min of growth to form continuous cone structures.

A nanofocused TEM-EDAX system was used to determine the elemental composition by scanning a line across the emitter to determine its elemental composition. Figure 4(a) shows the cross-sectional TEM image for elemental analysis, and the inset shows the measured area (the boundary between the substrate and the CNT). Figure 4(b) shows the magnified image of the rectangular area in Fig. 4(a). The difference in contrast is due to a difference in structure. The left side is the outer region and the right side is the silicon substrate. We can clearly see the amorphous phase in the outer region and a crystalline structure in the silicon substrate. For elemental composition analysis, the scan position of the TEM-EDAX system is depicted in Fig. 4(c); data were acquired from top to bottom. Figure 4(d) shows the relative count of silicon and carbon in the CNT. A high concentration of carbon was observed at the top position, but the concentration decreased with increasing scan length. The silicon at

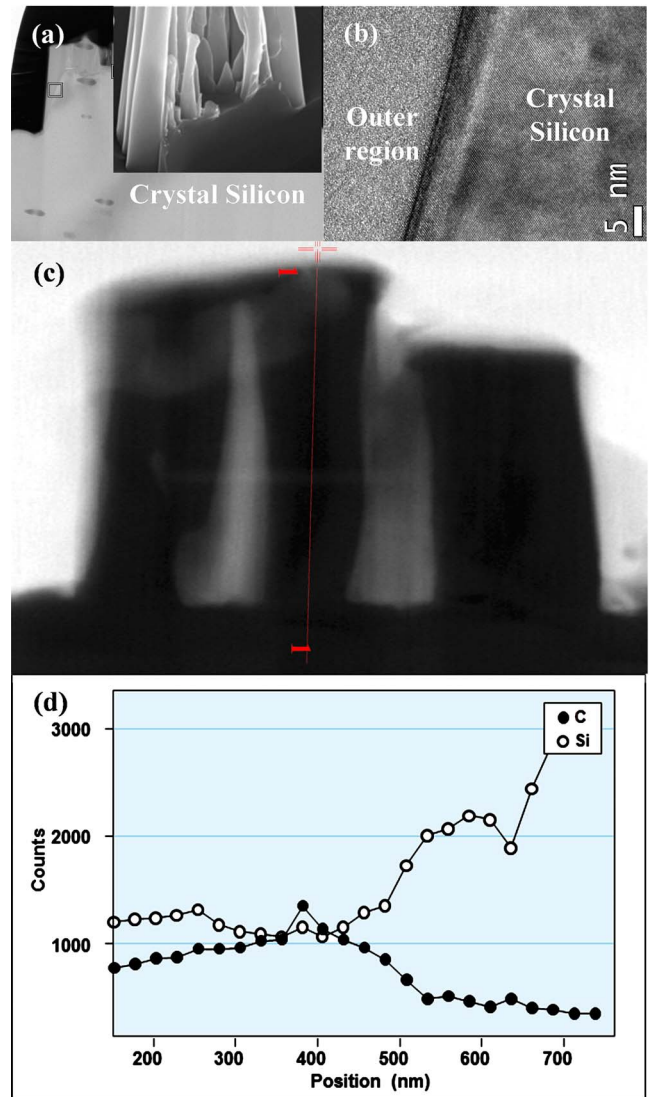


FIG. 4. (Color online) TEM images of vertically cross-sectioned silicon coated CNT emitters and elemental analysis along the CNT height. (a) A TEM image of the prepared sample and the sampling position (inset). (b) A high-resolution TEM image of the rectangular area in (a). (c) A TEM image and the scan line for the element analysis. (d) The relative concentration of carbon and silicon through the scan line.

the top position was amorphous silicon that surrounded the CNTs, whereas the increase in silicon at the bottom at the higher scan lengths was due to the substrate. We surmise that silicon comes from etching and diffusion of the silicon substrate followed by redeposition on the CNT surface. In the tip area, the silicon deposition rate may be low because of a higher concentration of hydrogen.

Figure 5 illustrates the silicon coated CNT emitter growth process. Figure 5(a) shows a cross section of aggregated Ni on the silicon substrate during the forming process. The diameter distribution of the agglomerated catalyst is similar to the diameters of the CNTs and ranges between 20 and 150 nm. Figure 5(b) shows CNTs grown for 30 min. However, the CNTs grown for 60 min and the robust CNT emitter in Fig. 5(c) were obtained. The structure can be obtained by

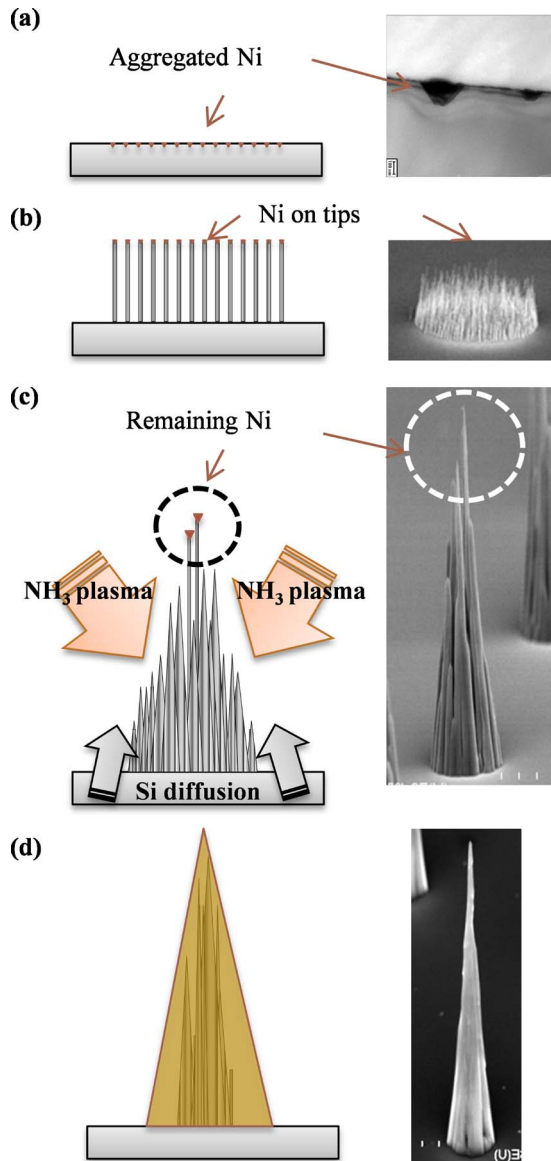


FIG. 5. (Color online) Schematic diagram of the silicon coated CNT emitter growth process. (a) Aggregation of the nickel catalyst after the high temperature forming process. (b) CNT growth in early growth stages (<30 min). (c) Robust CNT growth after 40 min growth time. (d) Silicon coated CNT growth. The CNT shows a nanometer-scaled tip apex and a micrometer-scaled base.

different silicon etch rates between the tip and the bottom areas. Some of the nickel catalyst are removed and stop further CNT growth, especially within the peripheral area. Silicon coated CNTs can be grown with increased growth temperature and time, as shown in Fig. 5(d).

Figure 6 shows the electron emission properties of the CNT emitters. Figure 6(a) shows the current-voltage characteristics in the dc mode. The field emission from CNT emitters deposited on Si substrates was measured by connecting the substrate to ground and applying a potential to the 3 mm diameter molybdenum anode placed 600  $\mu\text{m}$  away from the substrate. A CNT area measuring  $0.5 \times 0.5 \text{ cm}^2$  was used. Typically, tests began with base pressures in the  $10^{-7}$  Torr range. The anode assembly was supported by an insulated

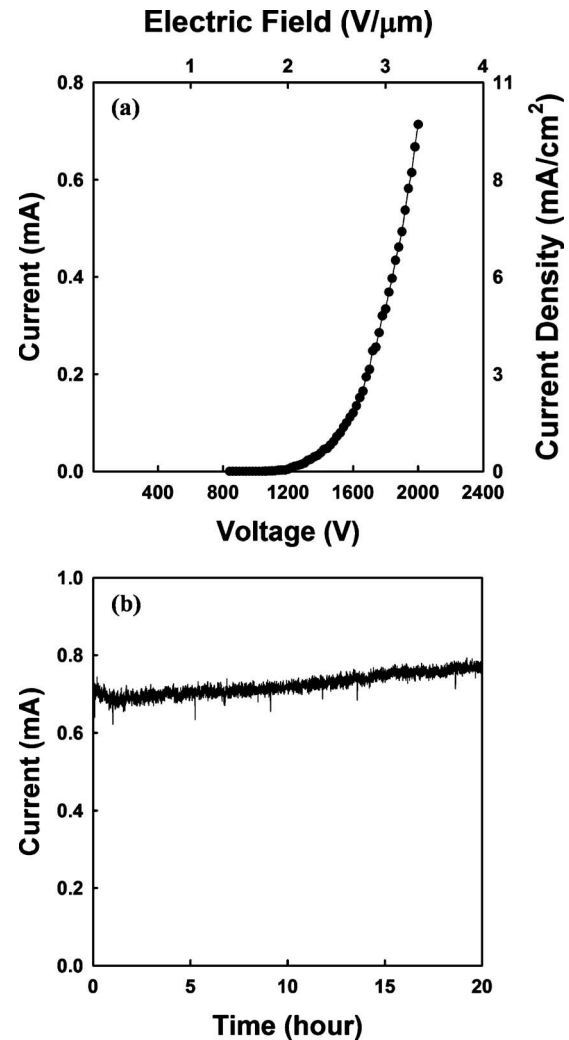


FIG. 6. (a) Electron emission properties and (b) emission current stability of the CNT emitters.

vacuum manipulator assembly that, for most measurements, positioned the anode 600  $\mu\text{m}$  away from the substrate. The turn-on field was 2  $\text{V}/\mu\text{m}$  at an emission current of 1  $\mu\text{A}/\text{cm}^2$ . However, non-silicon coated CNT emitters (less than 60 min growth time) grown with the RAP process show a threshold voltage range of 3–4  $\text{V}/\mu\text{m}$ .<sup>13</sup> The CNT emitters had a very sharp-tipped apex, which resulted in enhanced electron emission. Figure 6(b) shows the stability of the electron emission current of the silicon coated CNT emitters. Initially, the emission current was set at 0.7 mA (applied voltage=2000 V) in the dc mode. The emission current remained constant at approximately 0.7 mA for over 20 h of operation in the dc mode. We did not observe reduced emission current, rather the current rose to approximately 0.8 mA. The silicon coated CNT emitters showed enhanced and stabilized electron emission.

#### IV. CONCLUSIONS

We described a process for growing amorphous silicon coated CNT emitters using the RAP process. The CNT emit-

ters grown in this study showed several multiwall CNT structures with 130 graphene layers surrounded by an amorphous silicon coating. The CNT emitters had 3  $\mu\text{m}$  diameter bottom contacts with the silicon substrate and a cone-shaped sharp-tipped apex measuring a few nanometers in diameter. We obtained a turn-on field of 2 V/ $\mu\text{m}$  at an emission current of 1  $\mu\text{A}/\text{cm}^2$ , and the emission current was stable for at least 20 h. The silicon coated CNT emitter described in this paper is a potential candidate for high-performance electron emitters.

## ACKNOWLEDGMENTS

This work was supported by the National Research Foundation (Grant No. KRF-2009-013-C00018) and by a Kyung Hee University research grant in 2009 sabbatical.

<sup>1</sup>K. B. K. Teo, M. Chhowalla, G. A. J. Amaratunga, W. I. Milne, G. Pirio, P. Legagneux, F. Wyczisk, J. Olivier, and D. Pribat, *J. Vac. Sci. Technol.*

B **20**, 116 (2002).

<sup>2</sup>Z. Liu, G. Yang, Y. Z. Lee, D. Bordelon, J. Lu, and O. Zhou, *Appl. Phys. Lett.* **89**, 103111 (2006).

<sup>3</sup>S. Kita *et al.*, *J. Appl. Phys.* **103**, 064505 (2008).

<sup>4</sup>D. R. Whaley, B. M. Gannon, C. R. Smith, C. M. Armstrong, and C. A. Spindt, *Plasma Sci. Technol.* **28**, 727 (2000).

<sup>5</sup>E. Minoux *et al.*, *Nano Lett.* **5**, 2135 (2005).

<sup>6</sup>G. Cao *et al.*, *Phys. Med. Biol.* **54**, 2323 (2009).

<sup>7</sup>X. Calderón-Colón, H. Geng, B. Gao, L. An, G. Cao, and O. Zhou, *Nanotechnology* **20**, 325707 (2009).

<sup>8</sup>T. Y. Tsai, C. Y. Lee, N. H. Tai, and W. H. Tuan, *Appl. Phys. Lett.* **95**, 013107 (2009).

<sup>9</sup>K. C. Park, J. H. Ryu, K. S. Kim, Y. Y. Yu, and J. Jang, *J. Vac. Sci. Technol. B* **25**, 1261 (2007).

<sup>10</sup>J. H. Ryu, K. S. Kim, C. S. Lee, J. Jang, and K. C. Park, *J. Vac. Sci. Technol. B* **26**, 856 (2008).

<sup>11</sup>M. Jönsson, O. A. Nerushev, and E. E. B. Campbell, *Appl. Phys. A: Mater. Sci. Process.* **88**, 261 (2007).

<sup>12</sup>C. S. Lee, J. H. Ryu, H. E. Lim, K. W. Min, S. Manivannan, J. Jang, and K. C. Park, *J. Korean Phys. Soc.* **53**, 2735 (2008).

<sup>13</sup>S. H. Lim, K. C. Park, J. H. Moon, H. S. Yoon, D. Pribat, Y. Bonnassieux, and J. Jang, *Thin Solid Films* **515**, 1380 (2006).